


<https://doi.org/10.17221/135/2024-SWR>

Soil-water characteristic curves and related properties of disturbed forest soils

ADELA JOANNA HAMERNÍKOVÁ¹, PAVEL DLAPA^{1*}, SILVIA IHNAČÁKOVÁ¹,
ARTEMI CERDÀ², RÓBERT KANKA³, ĽUBOŠ HALADA³

¹Department of Soil Science, Faculty of Natural Sciences, Comenius University, Bratislava, Slovakia

²Soil Erosion and Degradation Research Group, Department of Geography, Valencia University, Valencia, Spain

³Institute of Landscape Ecology SAS, Bratislava, Slovakia

*Corresponding author: pavel.dlapa@uniba.sk

Citation: Hamerníková A.J., Dlapa P., Ihnačáková S., Cerdà A., Kanka R., Halada L. (2025): Soil-water characteristic curves and related properties of disturbed forest soils. *Soil & Water Res.*, 20: 143–152.

Abstract: Forest logging activities negatively affect various soil properties. In this study, we focus on the logging effects on soil water retention and associated pore size distribution. We measured the soil-water characteristic curves (SWCCs) on 21 undisturbed samples from three research plots: a reference area, a clear-cut area and a forest track. A total of 12 SWCC points between saturation and wilting point were determined for each sample with a sand box and pressure plate apparatus. The trimodal behaviour is highlighted by the dependence between soil moisture and suction. Therefore, we proposed a revised model by combining two exponential expressions with the van Genuchten model. The exponential terms describe the influence of macro-and-structural porosities, and the latter is used to calculate textural porosity. This new model with eight independent parameters was suitable to fit trimodal SWCCs in all samples. Results revealed that logging had the most destructive effect on large pores, and the soil on the forest track was the most affected. Both soil-air and available water capacity were reduced and the permanent wilting point increased as a result of damage to the soil structure and pore system. Observed increased organic carbon content in compacted soils can be attributed to slowed decomposition due to reduced air capacity and increased waterlogging susceptibility of damaged soils.

Keywords: forest logging; LTER Báb; pore size distribution; soil compaction; soil water retention; trimodal SWCC

It is generally assumed that forest soils are relatively stable, with low physical degradation, and therefore they have historically received less attention than agricultural soils. However, the following more recent research confirms that logging induces forest land degradation (Bowd et al. 2019; Marangon et al. 2024). Cambi et al. (2015) determined that the negative impacts of heavy machinery used in logging initially affect forest-soil porosity, and this disrupts other properties and processes. Their further investigation

recorded reduced soil micro-arthropod biodiversity and decreased seedling growth in compacted forest soils (Cambi et al. 2017). Herbauts et al. (1996) observed significantly reduced total porosity (TP) and decreased macropore volume below 10% in loamy topsoils in their assessed logging in Belgium. The authors also indicated decreased redox potential and significant hydromorphic processes in the compacted soils. Ampoorter et al. (2010) reported compaction's greater effect on soil aeration and CO₂ concentra-

Supported by the Science Grant Agency of the Slovak Republic VEGA, Projects No. 1/0703/23 and 2/0074/25.

© The authors. This work is licensed under a Creative Commons Attribution-NonCommercial 4.0 International (CC BY-NC 4.0).

tion than on bulk density (BD) values in loam to silt loam soils. Fründ and Averdiek (2016) observed CO₂ concentrations above 1% in silt loam soil compacted by the wheels of heavy machinery, which they linked to damaged soil structure. Hartmann et al. (2014) established that logging-induced compaction has a long-term impact on the soil's bacterial and fungal communities. Bellabarba et al. (2024) observed a higher resistance of the bacterial community to forest soil compaction in the short term compared to the fungal community. Frey et al. (2009) reported changes in bacterial community structure due to reduced macro-porosity and limited gas exchange in the compacted forest soils. Increasing soil BD has negative impact on plant morphology and physiology (Naghdi et al. 2016; Mariotti et al. 2020). Other authors recorded that tree removal and excess water also accelerated forest soil erosion. Borrelli et al. (2017) assessed that annual soil loss from water erosion was seven times greater in logged forests than in unaffected areas. Karami et al. (2023) observed a strong negative correlation between increased BD and runoff, sediment yield and nutrient loss. The negative impacts of forest harvesting on water quality in forested watersheds (increased sediment transport, concentrations of nutrients and organic carbon) were reviewed by Shah et al. (2022). Engler et al. (2024) summarized the environmental impacts of major forest harvesting systems in Europe. The impact of heavy machinery on forest land degradation is so severe that various mitigation measures have been proposed for harvesting operations (Labelle et al. 2022) and forestry best management practices are implemented (Hawks et al. 2022).

Although those negative logging impacts on forest soils relate to increased BD or reduced TP, some authors emphasize that changes in pore size distribution are more significant than the overall BD or TP changes. This is especially relevant to the soil macropore content (Herbauts et al. 1996; Ampoorter et al. 2010; Masumian et al. 2023). Knowledge of changes in pore size distribution (PSD) is also important in estimating the effect of compaction on hydrological and other soil properties.

Soil pore size distribution has recently been investigated in detail, especially in assessing the impact of agricultural land management and land use (Lipiec & Hatano 2003; Jensen et al. 2019; Sekucia et al. 2020). Those authors recorded that the PSD hierarchical nature can be derived from the soil-water characteristic curve (SWCC). However, similar advanced

SWCC analyses which apply multimodal PSD models are lacking in the current literature on forest logging effects. D'Acqui et al. (2020) investigated the porosity effect of forest soil compaction on the PSD inside the aggregates using mercury porosimetry, but without modelling. Furthermore, these measurements did not include interaggregate porosity. Therefore, we address this knowledge gap.

Herein, we evaluate the impact of logging with heavy machinery on forest soils. We employ detailed measurement of the soil-water characteristic curves at sites with different extents of logging damage. The curves' mathematical approximation elucidates the impact of logging on porosity and other researched soil properties.

MATERIAL AND METHODS

Study sites and soil sampling. The forest research area is located at the village of Báb, County of Nitra, SW Slovakia, Central Europe. The website (<https://deims.org/79e10639-dd60-4f30-9c43-7b2bae0f359a>) defines that the site is part of the Long-Term Ecological Research network (LTER). The area of the oak-hornbeam forest is 72.5 ha. The average annual temperature is 9–10 °C, while the average annual precipitation ranges from 500 to 600 mm. Research plots are in a 90-year-old forest, on a 3° slope with NE exposure, coordinates 48°18'13"N., 17°53'35"E. and an altitude of 180 m a. s. l.

The loess soils are classified as Cambic Chernozems (Loamic) (IUSS Working Group WRB 2022), and their properties are compared at a reference plot and two plots differently affected by logging (Figures 1 and 2). The trees were felled motor-manually by loggers using chainsaws. Extraction was then performed by a wheeled LKT81 forest tractor (manufactured by ZTS TEES, Martin, Slovakia) and a John Deere 1110E eight-wheel forwarder (Figure 2).

The surface part of the 40 cm thick humus horizon was examined. For this purpose, soil sampling from a depth of 0–10 cm was performed at the three plots: the reference area (unaffected forest), the clear-cut area, and the forest track (Figure 1). Seven undisturbed samples were randomly taken from each plot using 100 cm³ stainless steel cylinders. A 0–3 cm litter layer was removed prior to sampling.

Laboratory methods. The determination of SWCCs was as follows. Water-saturated samples in stainless steel cylinders were drained in several steps, and the soil moisture in equilibrium with the suction pres-

<https://doi.org/10.17221/135/2024-SWR>

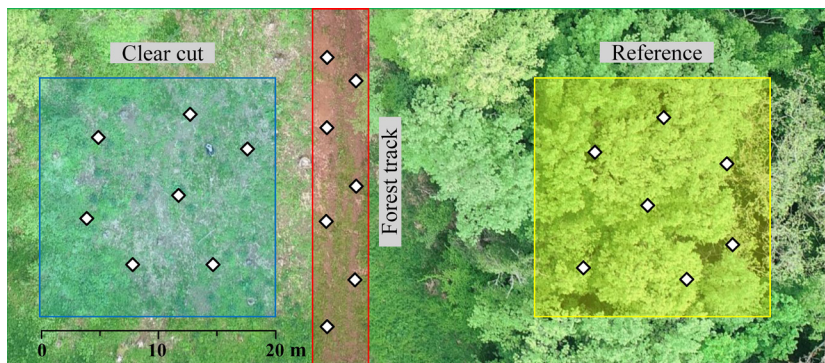


Figure 1. View of research plots differently affected by logging: clear cut (left), forest track (middle) and reference plot (right)

sure was recorded. Suctions of 0.3, 1, 3.1 and 10 kPa were applied in a sandbox (Eijkelkamp, Giesbeek, The Netherlands). A pressure plate extractor (Soilmoisture Equipment Corp., Santa Barbara, USA) was used for suctions of 41, 70, 100 and 131 kPa.

The soil samples were then air-dried, ground and sieved through a 2 mm sieve. The disturbed sub-sam-

ples were used to determine water retention at 310, 780 and 1 500 kPa in 1 cm high rubber rings, using the pressure plate extractor. The use of disturbed samples for high suction pressures was suggested by Jensen et al. (2019) to avoid errors caused by low hydraulic conductivity in cylinders with undisturbed samples. The samples were dried at 105 °C before



Figure 2. A wheeled forest tractor LKT81 (upper left) and a John Deere 1110E forwarder (upper right) during harvesting operations; view of the clear-cut plot (lower left) and the forest track (lower right)

determining the dry sample weight and BD. The total porosity (TP) was calculated from BD:

$$TP = 1 - BD/PD \quad (1)$$

where:

PD – the soil particle density determined by pycnometer method (Blake & Hartge 1986).

The air-dried sub-samples were used to determine pH in a soil-water suspension (1:2.5 w/v), the soil texture by pipette method (Gee & Or 2002), and the soil organic carbon (SOC) content by potassium dichromate oxidation (Nelson & Sommers 1996).

Statistical analysis. The SWCC model uses two exponential expressions to describe macro- and structural porosities and the van Genuchten (1980) expression for textural porosity:

$$\theta = C + A_1 \left[1 + (\alpha h)^n \right]^{(1/n-1)} + A_2 e^{(-h/h_2)} + A_3 e^{(-h/h_3)} \quad (2)$$

where:

θ – water content;

h – water suction;

C – residual water content;

$A_1, 1/\alpha, n$ – parameters in the van Genuchten term;

A_2, h_2, A_3, h_3 – parameters in the exponential terms.

A simple van Genuchten model was also used for comparison to avoid possible over-parameterised effects in Equation (2):

$$\theta = C + A \left[1 + (\alpha h)^n \right]^{(1/n-1)} \quad (3)$$

where:

A – equal to the difference between saturated and residual water content;

α, n – parameters in the van Genuchten model.

The SWCC includes information on pore size and volume. The pore diameter (μm) at a given suction is approximately $d \approx 3000/h$. This is based on the capillary equation, and the derivative of Equation (2) yields the pore size distribution:

$$\frac{d\theta}{d(\log h)} = -A_1(n-1)(\alpha h)^n \left[1 + (\alpha h)^n \right]^{(1/n-2)} \ln 10 - \frac{A_2}{h_2} e^{(-h/h_2)} h \ln 10 - \frac{A_3}{h_3} e^{(-h/h_3)} h \ln 10 \quad (4)$$

Python has the non-linear least-squares minimisation and curve fitting algorithm, and this LMFIT

for Python (Newville et al. 2022) was used to find the parameters in Equations (2) and (3). The Akaike information criterion (AIC) and root mean square error (RMSE) were calculated to evaluate the model's fit. The Akaike information criterion, corrected for the small sample size (AICc), was computed by the formula:

$$AICc = AIC + \frac{2k(k+1)}{n-k-1} \quad (5)$$

where:

k – the number of parameters and n is the number of samples.

Python software was also used to perform further statistical analyses. The differences between plots were tested using ANOVA followed by Tukey's test. The correlation coefficient was used to describe relationships between soil properties with statistical significance levels indicated as: *, **, *** $P \leq 0.05, 0.01, 0.001$.

RESULTS

The basic soil properties for individual research plots are summarised in Table 1. The soils range from clay loam in the reference area and forest track to silty clay loam in the clear-cut area. The reference area is characterized by a higher sand content, the clear-cut area has a higher clay content, and interestingly the forest track soil has the highest SOC. The slightly acid pH did not differ significantly at the three sites. In addition, the highest BD was found on the most affected forest track.

Table 1. Average soil properties with standard error ($n = 7$) for each plot

Parameter	Reference area	Clear-cut area	Forest track
pH	5.90 ± 0.25 ^a	6.03 ± 0.26 ^a	6.29 ± 0.04 ^a
SOC (%)	2.64 ± 0.24 ^a	2.95 ± 0.17 ^a	4.11 ± 0.17 ^b
Sand (%)	39.2 ± 3.1 ^a	17.9 ± 0.4 ^b	23.3 ± 0.7 ^b
Silt (%)	32.3 ± 2.1 ^a	46.3 ± 0.7 ^b	44.9 ± 1.2 ^b
Clay (%)	28.5 ± 1.2 ^a	35.8 ± 0.8 ^b	31.8 ± 0.9 ^a
PD (g/cm ³)	2.61 ± 0.01 ^a	2.62 ± 0.01 ^a	2.57 ± 0.01 ^b
BD (g/cm ³)	1.12 ± 0.01 ^{ab}	1.17 ± 0.05 ^b	1.25 ± 0.02 ^{bc}

SOC – soil organic carbon; PD – particle density; BD – bulk density; different letters indicate significant differences between plots ($P < 0.05$)

<https://doi.org/10.17221/135/2024-SWR>

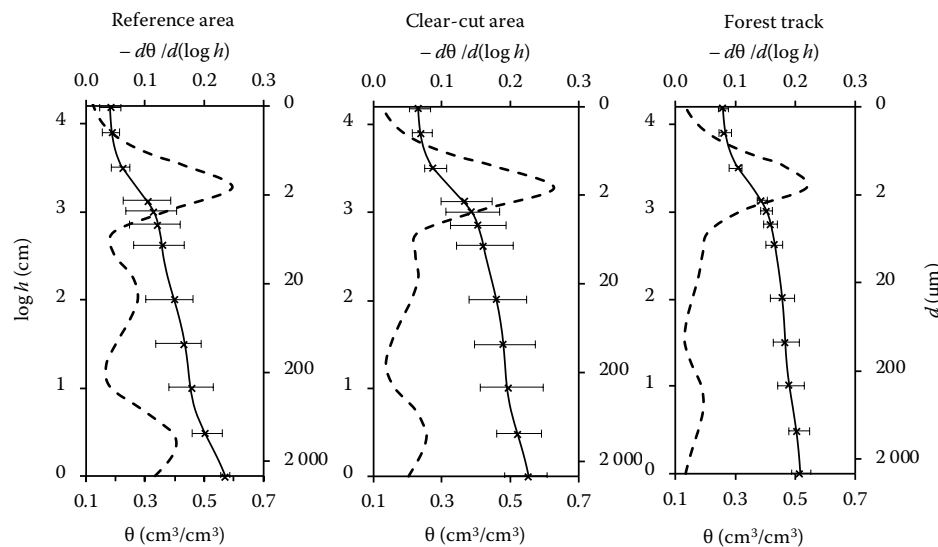


Figure 3. Average soil-water characteristic curves (solid line) and pore size distribution curves (dashed line) for each plot θ – water content; h – water suction; d – pore diameter; whiskers provide the min and max observed water contents

Figure 3 presents the SWCC measurement results, where the average values for each plot with the maximum and minimum values are indicated by whiskers. The SWCCs are multi-modal and the most compacted soils on the forest track have the least moisture variation throughout the $\log h$ range from 0 to 4.18.

Figure 3 also shows that the Equation (2) model perfectly describes the SWCC course at each of the three plots. While two exponential terms proved sufficient to express the dependence at the lower $\log h < 2.5$ suctions, the van Genuchten term describes the course of the curve at higher $\log h$ suctions. Table 2

summarises the parameters used for calculations depicted in Figure 3 (dashed lines). The trimodal PSD curves have three peaks with maxima between 485–1 329, 12–27 and 1.5–1.7 μm .

The Equation (3) model was also applied to water retention data for comparison (Table 3). Since the unimodal model provided negative values for the parameter C , residual moisture content, the values of the C parameter were thus fixed to the values provided by the trimodal model (Table 2). This model gives higher RMSE and AICc values than the trimodal Equation (2) in Table 2. The RMSE and AICc prove the validity of using the trimodal model.

Table 2. Parameters with standard error of the trimodal model (Equation 2) fitted to the average SWCCs for each plot

Parameter	Reference area	Clear-cut area	Forest track
C (cm^3/cm^3)	0.178 ± 0.005	0.227 ± 0.002	0.255 ± 0.002
A_1 (cm^3/cm^3)	0.178 ± 0.008	0.189 ± 0.006	0.170 ± 0.008
$1/\alpha$ (cm)	1541 ± 108	1546 ± 73	1747 ± 118
n	2.81 ± 0.25	2.82 ± 0.14	2.72 ± 0.15
A_2 (cm^3/cm^3)	0.103 ± 0.007	0.075 ± 0.004	0.047 ± 0.005
h_2 (cm)	110 ± 20	179 ± 33	258 ± 84
A_3 (cm^3/cm^3)	0.174 ± 0.013	0.088 ± 0.006	0.053 ± 0.003
h_3 (cm)	2.26 ± 0.33	2.85 ± 0.40	6.19 ± 0.89
RMSE (cm^3/cm^3)	$2.51\text{E}-03$	$1.29\text{E}-03$	$9.20\text{E}-04$
AICc	-79.7	-95.6	-103.8

SWCCs – soil-water characteristic curves; C – residual moisture, A_1 , $1/\alpha$, n – parameters in the van Genuchten term, A_2 , h_2 , A_3 , h_3 – parameters in the exponential terms; RMSE – the root mean square error; AICc – the Akaike's information criterion with correction for the small sample size

Table 3. Parameters with standard error of the van Genuchten model (Equation 3) fitted to the average SWCCs for each plot

Parameter	Reference area	Clear-cut area	Forest track
C (cm ³ /cm ³)	0.178	0.227	0.255
A_1 (cm ³ /cm ³)	0.347 ± 0.032	0.273 ± 0.013	0.228 ± 0.009
A (1/cm)	0.0532 ± 0.0565	0.0018 ± 0.0006	0.0013 ± 0.0003
n	1.28 ± 0.08	1.85 ± 0.27	1.94 ± 0.25
RMSE (cm ³ /cm ³)	3.70E–02	2.42E–02	1.73E–02
AICc	–70.1	–80.3	–88.3

SWCCs – soil-water characteristic curves; C , A – the volumetric water contents; α – the parameter roughly corresponding to the inverse of the air-entry value; n – the empirical shape-defining parameter; RMSE – the root mean square error; AICc – the Akaike's information criterion with correction for the small sample size

The water retention calculated in each sample using the Equation 2 model is controlled by pore size distribution (Figure 4). The largest pores drained at $\log h < 1.80$ determine the soil air capacity (AC). Similar to the macropore contents, the AC decreased in an order of reference plot > clear-cut plot > forest track. The available water capacity (AWC) for $\log h$ between 1.80 and 4.18 was highest in the clear-cut plot, but differences were not significant. The permanent wilting point (PWP) at $\log h$ 4.18 was highest at the forest track, followed by the clear-cut and reference plots.

DISCUSSION

Multi-modal pore distribution. There is a need to differentiate between pore categories when analysing water retention properties from full saturation

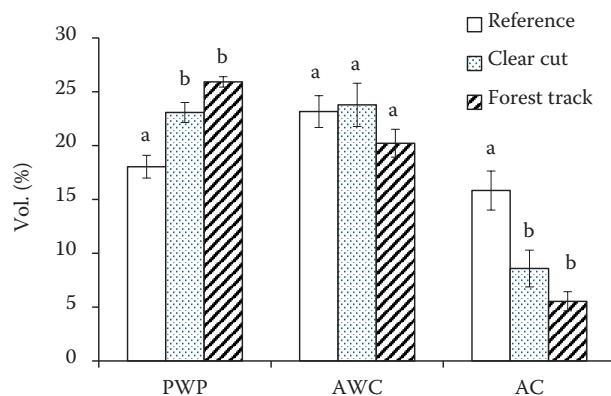


Figure 4. Average permanent wilting point (PWP), available water capacity (AWC) and air capacity (AC) for each plot ($n = 7$)

Whiskers present the standard errors and letters indicate significant differences between plots ($P < 0.05$)

to residual moisture (Kutílek et al. 2006; Dexter et al. 2008; Jensen et al. 2019; Dłapa et al. 2020). Santos et al. (2011) also stresses the importance of macropores, because these often escape attention in analysing the results of water retention experiments. Kutílek et al. (2006) reported the importance of distinguishing matrix (textural) and structural porosity in their compression experiments.

Several authors have successfully applied bimodal models to water retention data. These include Durner's use of the van Genuchten bimodal model (Durner 1994), while other authors employ the Kosugi bimodal function (Kutílek et al. 2006; Fernández-Gálvez et al. 2021). Jensen et al. (2019) successfully applied Dexter's double-exponential model on soils with clay content of 2 to 30 wt.% (Dexter et al. 2008).

The existence of macropores, textural and structural pores indicates that trimodal models are required to fit more complex courses of the θ vs. $\log h$ dependence (Dexter & Richard 2009; Sekucia et al. 2020). Herein, using a greater number of points showed that even the bimodal model is insufficient (Figure 3). The double-exponential model has a small number of parameters, so we extended this by the van Genuchten function. The resulting trimodal model has 8 independent parameters, and the RMSE and AICc values in Table 2 confirm its suitability.

D'Acqui et al. (2020) used mercury porosimetry to determine PSD in loamy aggregates. Their measurement did not include pores larger than 200 μm . Interestingly, they found two maxima in the range of 1–2.5 and 10–25 μm that agree well with maxima 1.5–1.7 and 12–27 μm observed in our PSD curves (Figure 3). Heavy mechanisms reduced pore volume mainly between 7–50 μm in the work of D'Acqui et al. (2020), which corresponds well to the decrease in the middle peak in Figure 3 for the clear-cut area and

<https://doi.org/10.17221/135/2024-SWR>

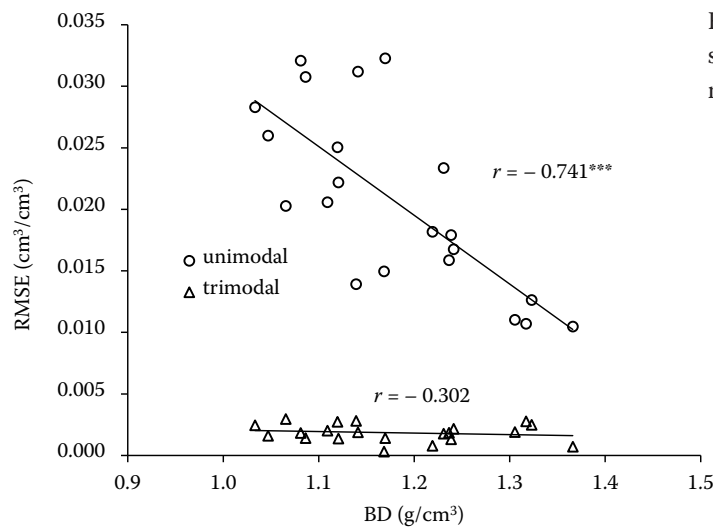


Figure 5. Standard deviation of residuals (root mean square error, RMSE) versus bulk density (BD) of unimodal and trimodal models in all samples

forest track. In addition, we observed a significant decrease in the peak of the largest pores with maxima in the range of 485–1329 μm .

Figure 5 highlights how model error depends on BD when the trimodal or unimodal model is employed. Soils less affected by compaction have a more preserved structure and more pronounced trimodal effect, so the simple van Genuchten model is therefore less accurate.

Santos et al. (2011) and Kutílek et al. (2006) showed that soil compaction affects characteristic suctions or idealised equivalent pore sizes in specific pore categories. In our samples, soil compaction results in decreased macro- and structural pore volume, which is accompanied by reduced pore size (Figure 3). Kutílek et al. (2006) observed a similar reduction in compressed sandy clay loam soil. Our Chernozem

has a well-developed stable structure, and the decrease in equivalent pore diameters (or increased suctions h_2 and h_3 in Table 2) concurs with Kutílek et al. (2006) interpretation for soils with a stable structure.

Aeration and water retention. We used the neural network prediction to assess possible influence of soil texture on porosity (Rosetta Lite Ver. 1.1) (Schaap et al. 2001; Ma et al. 2024). Predicted values for three research plots (Table 1) showed an order: clear cut > forest track > reference plot for TP values (0.56 > 0.54 > 0.49). The average values actually determined in the soils follow in a different order: reference plot > clear cut > forest track (0.57 > 0.55 > 0.52). These relative differences suggest that compaction-induced changes have a greater impact than soil texture.

However, not all pores have the same change in volume. Figure 6 depicts the relationship between pore

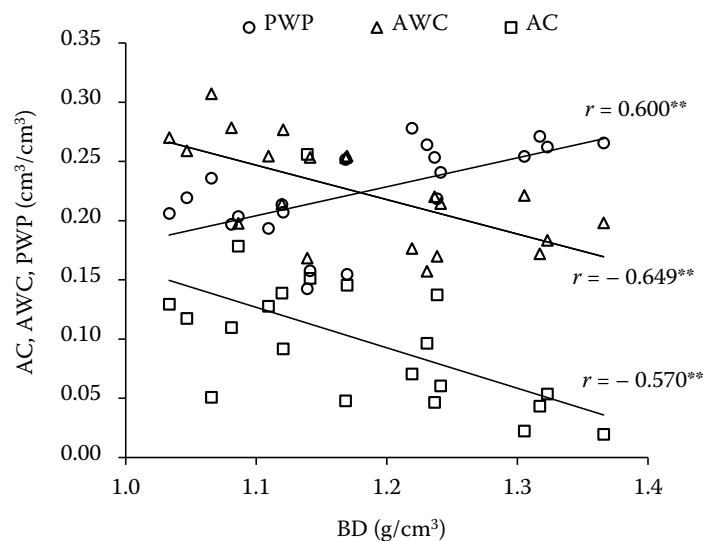


Figure 6. Air capacity (AC), available water capacity (AWC) and permanent wilting point (PWP) versus bulk density (BD) in all samples

properties and BD, and this shows that compaction induces a comparable decrease in the volume of pores responsible for soil AC and available water capacity. On the contrary, increased soil BD is accompanied by increased PWP which represents residual porosity.

Interestingly, the soil within the forest track has relatively low BD values and the BD increase in relation to the reference area is 11.6% only (Table 1). Compacted forest soils affected by heavy mechanization rarely show such low values of bulk density and compaction percentage (Mariotti et al. 2020). Observed resistance to compaction may be related to the very good structural stability of the investigated forest Chernozem. The soils have a high content of stable organic matter with a predominance of humic acids, and research by other authors has also shown a significantly higher content of stable aggregates compared to agricultural soils at this location (Polláková et al. 2018).

Although BD increased by 4.5% in our clear-cut area and by 11.6% on the forest track, changes in the pore distribution were more pronounced when AC on these two plots decreased by 46% and 65% respectively (Figure 4). This concurs with Ampoorter et al. (2010) who concluded that CO₂ concentration is a more sensitive indicator of soil compaction than of BD. Fründ and Averdick (2016) also reported impaired aeration at a depth of 5–7 cm in compacted forest soils.

The reduced volume of pores responsible for AC and AWC also results in decreased soil water permeability. The impaired natural dynamics of drying and wetting in compacted forest soil was reported by Fründ and Averdick (2016). The water in the pores limits oxygen supply and slows microbial decomposition of organic matter. These combined effects may be responsible for higher SOC content at our forest track, because it was used by cars and forestry equipment long before logging began.

Logging in forest lands can result in damages that contribute to the degradation of the soils through water logging and also increase soil erosion. Those findings show that logging can reduce the sustainability of the soils in forest land and affect the land degradation neutrality and the sustainable development goals of the United Nations (Keesstra et al. 2016).

CONCLUSION

The investigated forest soils exhibited trimodal behaviour of the SWCCs. Therefore, a revised model

was proposed that included two exponential expressions for macro-and-structural porosities and the van Genuchten expression for textural porosity. This model with eight independent parameters was suitable for approximating SWCC and evaluating the pore size distribution in all samples.

Compaction in the upper 10 cm of the soil affected by logging was evident during sampling in the clear-cut area and most pronounced on the forest track. The SWCCs revealed that logging with heavy machinery had a decisive effect on reducing the volume of large pores. The AC and AWC thus decreased, while the PWP increased in compacted soils. The decrease in the volume of macro- and structural pores was accompanied by a decrease in their equivalent diameters.

The higher SOC in the most compacted soils can be attributed to reduced soil AC and increased susceptibility to waterlogging, as these changes slow down the organic matter decomposition.

REFERENCES

- Ampoorter E., Van Nevel L., De Vos B., Hermy M., Verheyen K. (2010): Assessing the effects of initial soil characteristics, machine mass and traffic intensity on forest soil compaction. *Forest Ecology and Management*, 260: 1664–1676.
- Bellabarba A., Giagnoni L., Adessi A., Marra E., Laschi A., Neri F., Mastrodonato G. (2024): Short-term machinery impact on microbial activity and diversity in a compacted forest soil. *Applied Soil Ecology*, 203: 105646.
- Blake G.R., Hartge K.H. (1986): Particle density. In: Klute A. (ed.): *Methods of Soil Analysis. Part 1. Physical and Mineralogical Methods*. Madison, ASA: 377–382.
- Borrelli P., Panagos P., Märker M., Modugno S., Schütt B. (2017): Assessment of the impacts of clear-cutting on soil loss by water erosion in Italian forests: First comprehensive monitoring and modelling approach. *Catena*, 149: 770–781.
- Bowd E.J., Banks S.C., Strong C.L., Lindenmayer D.B. (2019): Long-term impacts of wildfire and logging on forest soils. *Nature Geoscience*, 12: 113–118.
- Cambi M., Certini G., Neri F., Marchi E. (2015): The impact of heavy traffic on forest soils: A review. *Forest Ecology and Management*, 338: 124–138.
- Cambi M., Hoshika Y., Mariotti B., Paoletti E., Picchio R., Venanzi R., Marchi E. (2017): Compaction by a forest machine affects soil quality and *Quercus robur* L. seedling performance in an experimental field. *Forest Ecology and Management*, 384: 406–414.

<https://doi.org/10.17221/135/2024-SWR>

- D'Acqui L.P., Certini G., Cambi M., Marchi E. (2020): Machinery's impact on forest soil porosity. *Journal of Terramechanics*, 91: 65–71.
- Dexter A.R., Richard G. (2009): The saturated hydraulic conductivity of soils with n-modal pore size distributions. *Geoderma*, 154: 76–85.
- Dexter A.R., Czyz E.A., Richard G., Reszkowska A. (2008): A user-friendly water retention function that takes account of the textural and structural pore spaces in soil. *Geoderma*, 143: 243–253.
- Dlapa P., Hriník D., Hrabovský A., Šimkovic I., Žarnovičan H., Sekucia F., Kollár J. (2020): The impact of land-use on the hierarchical pore size loamy soils. *Water*, 12: 339.
- Durner W. (1994): Hydraulic conductivity estimation for soils with heterogeneous pore structure. *Water Resources Research*, 30: 211–223.
- Engler B., Hartmann G., Mederski P.S., Bont L.G., Picchi G., Alcoverro G., Purfürst T., Schweier J. (2024): Impact of forest operations in four biogeographical regions in Europe: Finding the key drivers for future development. *Current Forestry Reports*, 10: 337–359.
- Fernández-Gálvez J., Pollacco J.A.P., Lilburne L., McNeill S., Carrick S., Lassabatère L., Angulo-Jaramillo R. (2021): Deriving physical and unique bimodal soil Kosugi hydraulic parameters from inverse modelling. *Advances in Water Resources*, 153: 103933.
- Frey B., Kremer J., Rüdert A., Sciacca S., Matthies D., Lüscher P. (2009): Compaction of forest soil with heavy logging machinery affects soil bacterial community structure. *European Journal of Soil Biology*, 45: 312–320.
- Fründ H.-C., Averdick A. (2016): Soil aeration and soil water tension in skidding trails during three years after trafficking. *Forest Ecology and Management*, 380: 224–231.
- Gee G.W., Or D. (2002): Particle-Size analysis. In: Dane J.H., Topp G.C. (eds.): *Methods of Soil Analysis. Part 4. Physical Methods*. Madison, SSSA: 255–293.
- Hartmann M., Niklaus P.A., Zimmermann S., Schmutz S., Kremer J., Abarenkov K., Lüscher P., Widmer F., Frey B. (2014): Resistance and resilience of the forest soil microbiome to logging-associated compaction. *The ISME Journal*, 8: 226–244.
- Hawks B.S., Aust W.M., Bolding M.C., Barrett S.M., Schilling E.B., Prisley S.P. (2022): Increased levels of forestry best management practices reduce sediment delivery from middle and lower coastal plain clearcut harvests and access features, southeastern states, USA. *Forest Ecology and Management*, 519: 120323.
- Herbauts J., El Bayad J., Gruber W. (1996): Influence of logging traffic on the hydromorphic degradation of acid forest soils developed on loessic loam in middle Belgium. *Forest Ecology and Management*, 87: 193–207.
- IUSS Working Group WRB (2022): World Reference Base for Soil Resources. International soil classification system for naming soils and creating legends for soil maps. 4th Ed. Vienna, International Union of Soil Sciences (IUSS).
- Jensen J.L., Schjonning P., Watts C.W., Christensen B.T., Munkholm L.J. (2019): Soil water retention: Uni-Modal models of pore-size distribution neglect impacts of soil management. *Soil Science Society of America Journal*, 83: 18–26.
- Karami S., Jourgholami M., Attarod P., Venanzi R., Latterini F., Stefanoni W., Picchio R. (2023): The medium-term effects of forest operations on a mixed broadleaf forest: Changes in soil properties and loss of nutrients. *Land Degradation & Development*, 34: 2961–2974.
- Keesstra S.D., Bouma J., Wallinga J., Tittonell P., Smith P., Cerdà A., Montanarella L., Quinton J.N., Pachepsky Y., van der Putten W.H., Bardgett R.D., Moolenaar S., Mol G., Jansen B., Fresco L.O. (2016): The significance of soils and soil science towards realization of the United Nations Sustainable Development Goals. *Soil*, 2: 111–128.
- Kutilek M., Jendele L., Panayiotopoulos K.P. (2006): The influence of uniaxial compression upon pore size distribution in bi-modal soils. *Soil and Tillage Research*, 86: 27–37.
- Labelle E.R., Hansson L., Högbom L., Jourgholami M., Laschi A. (2022): Strategies to mitigate the effects of soil physical disturbances caused by forest machinery: A comprehensive review. *Current Forestry Reports*, 8: 20–37.
- Lipiec J., Hatano R. (2003): Quantification of compaction effects on soil physical properties and crop growth. *Geoderma*, 116: 107–136.
- Ma L., Wang S., Ni C., Wang W., Kang S., Li Z., Wright A.L., Jiang X. (2024): Measurement and modelling of soil water dynamics under ridge tillage in paddy field. *Soil and Tillage Research*, 244: 106172.
- Marangon D., Betetto C., Wohlgemuth T., Cadez L., Alberti G., Tomelleri E., Lingua, E. (2024): Impact of salvage logging on short-term natural regeneration in montane forests of the Alps after large windthrow events. *Forest Ecology and Management*, 567: 122085.
- Mariotti B., Hoshika Y., Cambi M., Marra E., Feng Z., Paoletti E., Marchi E. (2020): Vehicle-induced compaction of forest soil affects plant morphological and physiological attributes: A meta-analysis. *Forest Ecology and Management*, 462: 118004.
- Masumian A., Rabiee M.R.S., Solgi A., Behjou F.K., Marchi E., Hájek M., Weisi L., Geraeli H. (2023): Assessment of the impact of ground-based skidding on soil physical properties: Initial effect and medium-term recovery. *International Journal of Forest Engineering*, 35: 284–295.

- Naghdi R., Solgi A., Labelle E.R., Zenner E.K. (2016): Influence of groundbased skidding on physical and chemical properties of forest soils and their effects on maple seedling growth. *European Journal of Forest Research*, 135: 949–962.
- Nelson D.W., Sommers L.E. (1996): Total carbon, organic carbon, and organic matter. In: Sparks D.L., Page A.L., Helmke P.A., Loeppert R.H., Soltanpour P.N., Tabatabai M.A., Johnston C.T., Sumner M.E. (eds.): *Methods of Soil Analysis. Part 3. Chemical Methods*. Madison, SSSA: 961–1010.
- Newville M., Otten R., Nelson A., Stensitzki T., Ingarciola A., Allan D., Fox A., Carter F., Michał, Osborn R., Pustakhod D., Ineuhaus, Weigand S., Aristov A., Glenn, Deil C., Mark, Hansen A.L.R., Pasquevich G., Foks L., Zobrist N., Frost O., Stuermer, azelcer, Polloreno A., Persaud A., Nielsen J.H., Pompili M., Caldwell S., Hahn A. (2022): *lmfit/lmfit-py: 1.1.0*. Zenodo. Available on <https://doi.org/10.5281/zenodo.7370358> (accessed Feb 8, 2023).
- Polláková N., Šimanský V., Kravka M. (2018): The influence of soil organic matter fractions on aggregates stabilization in agricultural and forest soils of selected Slovak and Czech hilly lands. *Journal of Soils and Sediments*, 18: 2790–2800.
- Santos G.G., da Silva E.M., Marchão R.L., da Silveira P.M., Bruand A., Becquer T. (2011): Analysis of physical quality of soil using the water retention curve: Validity of the S-index. *Comptes Rendus Geoscience*, 343: 295–301.
- Schaap M.G., Lei F.J., van Genuchten M.T. (2001): Rosetta: A computer program for estimating soil hydraulic parameters with hierarchical pedotransfer functions. *Journal of Hydrology*, 251: 163–167.
- Sekucia F., Dlapa P., Kollár J., Cerdá A., Hrabovský A., Svobodová L. (2020): Land-use impact on porosity and water retention of soils rich in rock fragments. *Catena*, 195: 104807.
- Shah N.W., Baillie B.R., Bishop K., Ferraz S., Högbom L., Nettles J. (2022): The effects of forest management on water quality. *Forest Ecology and Management*, 522: 120397.
- van Genuchten M.T. (1980): A closed-form equation for predicting the hydraulic conductivity of unsaturated soils. *Soil Science Society of America Journal*, 44: 892–898.

Received: November 5, 2024

Accepted: March 21, 2025

Published online: April 7, 2025